INTERNATIONAL JOURNAL OF PRECISION ENGINEERING AND MANUFACTURING Vol. 19, No. 8, pp. 1115-1124 AUGUST 2018 / 1115

REGULAR PAPER

DOI: 10.1007/s12541-018-0132-x
ISSN 2234-7593 (Print) / 2005-4602 (Online)

Experimental Investigation of Dynamic Errors in Coordinate Measuring Machines for High Speed Measurement

Younes Echerfaoui[1], Abderrazak El Ouafi[1,#], and Ahmed Chebak[1]

1 Department of Mathematics, Computer and Engineering, University of Quebec at Rimouski, Rimouski, G5L 3A1, Canada
Corresponding Author / E-mail: Abderrazak_elouafi@uqar,ca, TEL: +1-418-723-1986
ORCID: 0000-0002-1455-6507

KEYWORDS: Coordinate measuring machine, High-speed measurement, Dynamic errors, Laser interferometer, Design of experiments, Error compensation

Accuracy enhancement of coordinate measuring machine (CMM) by software compensation for geometric and thermal error has proved its effectiveness in the modern manufacturing. In some applications, measurement errors can be reduced by more than 70% when using error compensation. However, due to the demand for shorter cycle times of measurement tasks, CMMs are increasingly required to be used at high measuring velocity. In such conditions, dynamic errors will certainly have a much more influence on the measurement accuracy and constitutes a barrier to the reduction of measuring cycle time. This paper presents an experimental investigation of dynamic errors in CMMs. A structured experimental design and improved statistical analysis tools are combined to evaluate the measurement parameters effects at high measuring velocity. Carried out on a bridge type CMM, these parameters are combined and used to investigate the variation of several dynamic error attributes. A laser interferometer system is used to assess error components under different dynamic conditions. Based on these results, the contributions of each parameter in the variation of the dynamic error attributes are estimated revealing many options to consider for building an efficient prediction model for error compensation. Neural network based prediction model suggests a promising performance.

Manuscript received: November 24, 2017 / Revised: May 14, 2018 / Accepted: May 28, 2018

NOMENCLATURE

MPE = Maximum positioning error
RPE = Residual positioning error
MAE = Maximum approaching error
RAE = Residual approaching error
% C = Percent contribution
F = Fisher test

1. Introduction

Coordinate Measuring Machines, often called CMMs, are multi-axis machines widely used in industry to evaluate dimensional and geometric characteristics of complex high precision parts. A common but inadequate industrial practice is to assume any part measurement to be nearly error free or in the worst case to be within CMM volumetric error specifications provided by the CMM manufacturer or obtained by a calibration. This oversimplification of the CMM precision is often misleading since several factors are involved. In addition, with the development of computer-integrated manufacturing systems, the need for more complex products, the miniaturization of mechanical components, the demand for shorter cycle times and the guaranteed quality of the product are becoming increasingly pressing requirements.[1,2] In response to these findings, two imminent trends in the development of CMMs are emerging: higher measuring accuracy and higher measuring velocity.

When considering the accuracy of multi-axis machines such as CMMs, the sources of quasi-static errors can be identified: geometric errors due to the limited accuracy of the components, such as guideways and measurement systems, and thermal errors such as expansion and bending of machine components due to uniform temperature changes

Table 1 Typical coordinate measuring machine measurement errors

Error sources		Measurement errors
Machine Structure	Geometric	Typically between 4 and 30 μm
	Thermal	Typically between 6 and 12 μm/ °C/meter
Probing system	Approach direction, probe length, stylus radius, …	Typically < 2 μm (can reach 10 μm)
Software	Processing algorithms	Often < 2 μm
Dynamic errors	Velocity, acceleration, vibrations, …	Typically between 2 and 8 μm (can exceed 25 μm)

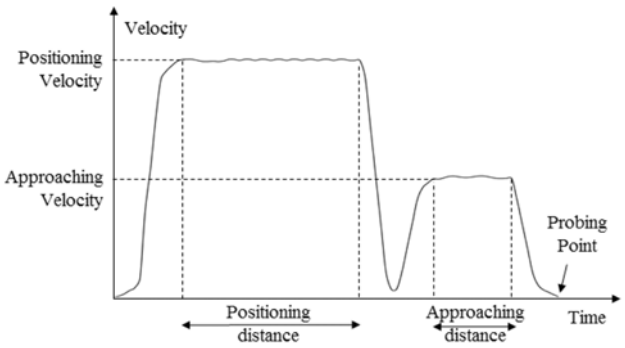

Fig. 1 Measurement process of touch-trigger probing

and temperature gradients. Results reported in the literature indicate typical quasi-static errors reaching up to 50 mm for commonly used CMM. The measurement errors introduced by the probing system and by the software deteriorate the performance of the CMM by about 1 to 10 mm overall. These errors are increased by other parameters such as positioning and probing speed, acceleration and direction. Typical CMM measurement errors are presented in Table 1. The reduction of the quasi-static errors involves the measurement of all the errors and the implementation of software error compensation. This method is an economical and effective way to improve the measuring accuracy.[2-8] From Table 1, it is clear that the CMM structural error dominates. It was thus natural to begin the investigation and the development of a compensation system addressing this problem. As result, the error compensation technique is currently accepted by more and more people and is applied successfully to compensate for geometric errors and thermal errors.[3-16] However, as the velocity of CMMs increases, dynamic errors significantly impact measurement. The assessments of these dynamic errors are quite limited.[16,17]

Generally, dynamic errors are caused by machine dynamics which may vary from one type of CMM to the other. Dynamic errors are reliant on machine structural properties such as mass distribution, component stiffness and damping characteristics, on dynamic factors like velocity and acceleration dependent deformation of the machine components due to motions and vibrations, both self-induced and forced, as well as on control parameters and disturbing forces. Therefore, the increase in measuring velocities in CMM applications is limited by dynamic errors amplitudes.

As the necessity to improve the working accuracy of CMMs in high velocity measuring conditions is well recognized, the question then arises as to the best way to achieve it. Dynamic error compensation is much more complicated than geometric and thermal errors compensation. Some studies on dynamic errors can be seen in Refs. 18-24. Until now, however, investigations of dynamic errors of CMMs are still inadequate, and effective approaches are needed to reduce the dynamic errors of CMMs.

During the high velocity measuring process in a CMM, the value and direction of the accelerations change constantly producing very large disturbing forces because of the mass involved. The dynamic errors caused by these forces have a great influence on the measuring accuracy. The purpose of this paper is to conduct an experimental investigation in order to characterize the dynamic error properties caused by high velocity effects and various measurement parameters and conditions. Carried out on a bridge-type CMM using a touch-trigger probe, this experimental study is used to identify the key factors that have the most effects on the dynamic errors, to include in a practical method for predicting and compensating for dynamic errors.

2. Dynamic Errors of CMMS due High-Speed Measuring Conditions

There are many factors that influence the cycle time of a measuring task and have an impact on the measuring accuracy. These factors include: positioning / approaching speed, positioning / approaching acceleration / deceleration, and positioning / approaching distances. The relation between these factors and the dynamic errors depends on the measuring task itself. When a measurement is carried out with a touch-trigger probe, usually the probe travels a small approaching distance at a low velocity before probing, while the positioning velocity between probing points can be very high. The velocity change in a typical point measurement is shown in Fig. 1. The small distance before the probing point is called the approaching distance. The dynamic errors are then aggravated by several parameters and are difficult to be assessed. Therefore, they cannot be compensated for by simply using the kinematic model as for static error compensation.

The used pattern of motion greatly affects the cycle time of the measurement task as well as the accuracy. Fig. 2 describes typical motion pattern indicating the acceleration, the velocity and the dynamic positioning error of the probe versus time. When the velocity changes, acceleration and inertial forces provoke dynamic positioning errors and, if probing during this time, introduce measurement errors. To avoid these undesirable dynamic errors, a delay between decelerating and probing is necessary to allow the acceleration and the inertial forces effects to decrease. However, this is not often possible in practice. The CMM will still be in acceleration / deceleration when contacting the measuring part especially for short approaching distances. This is often the case for small measuring parts when the approaching distances are very short and the CMM can be subject to disturbing forces during the probing time. When the approaching distance increases, the deformation and oscillation will be damped out before probing.

For static and geometric error compensation, the error budget can be treated as functions of the coordinates of the CMM. Dynamic errors are more complex and therefore involve more parameters. As illustrated in Figs. 1 and 2, these parameters include: geometric parameters (coordinate of the point to be measured and probing direction), control

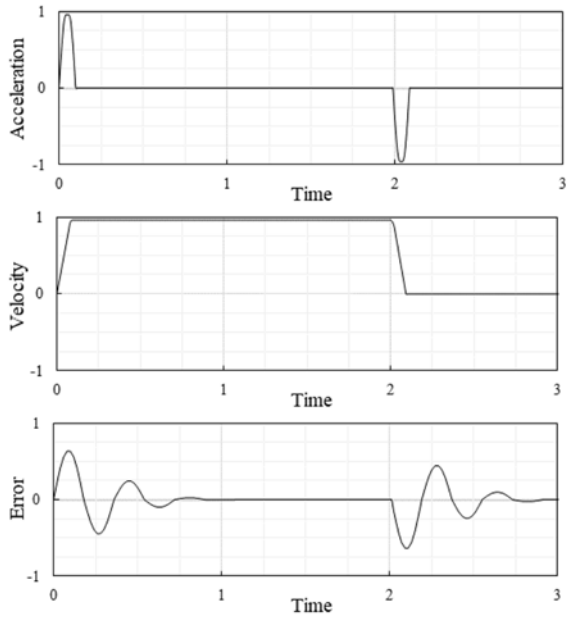

Fig. 2 Graphic illustration of typical motion pattern during the measurement process using normalized measures

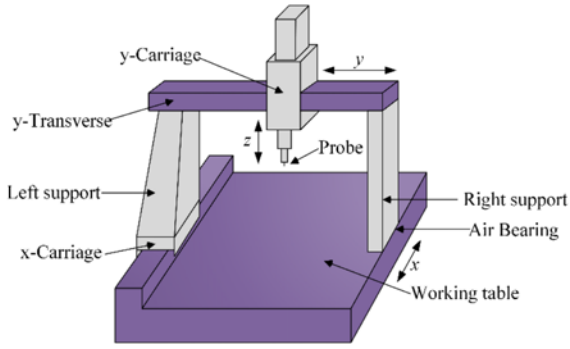

Fig. 3 Structure of the bridge-type coordinate measuring machines

parameters (positioning velocity, positioning acceleration, approaching velocity, approaching acceleration, positioning distance and approaching distance).

In the case of bridge-type CMM illustrated in Fig. 3, large inertial forces are produced on the structure of the machine during acceleration / deceleration due to the distributed mass of components. Since the driving system is located on one side of the bridge and because of the limited stiffness of the air bearings, the bridge have rotational motion around the joints of air bearings. The bridge also exhibits elastic deformation under the pressure of inertial forces. These rotational errors result in translation errors at the probe because of the Abbe offset in the x direction. In addition to these rotational errors, oscillations are also present due to machine dynamics.[24,25] To identify the contribution of each error source in the global dynamic error, a laser interferometer is used to evaluate the deformation of CMM components under various dynamic conditions. Translational and rotational errors as well as probe position are measured to reflect these contributions and therefore the structural deformation under various dynamic conditions.

As mentioned above, the pattern of motion affects the cycle time of

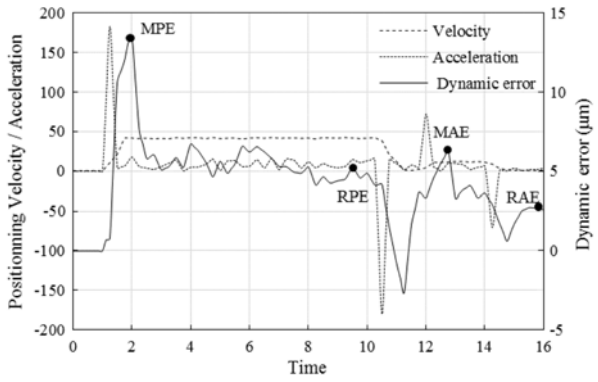

Fig. 4 Definition of dynamic error attributes

the measurement task as well as the accuracy. To maximize the productivity of the CMM, it is necessary to search for minimizing the measurement time. This can be achieved by increasing the positioning velocity and the measuring velocity and by reducing the positioning distance and the approaching distance. This is only possible if the dynamic error can be evaluated according to all the measurement parameters. For this reason, several attributes of the dynamic error have been defined in order to follow the error variation at different stages of the adopted measurement pattern from start to stop and to understand how the measurement parameters affect the error variation.

Fig. 4 shows the velocity and acceleration changes in a typical point measurement using a laser interferometer time-based measurement on a bridge-type CMM equipped with Renishaw touch-trigger probe under different tow sets parameters. In this pattern of motion, the positioning velocity is 40 mm/s and the measuring velocity is 12 mm/s. The dynamic error changes from 3 to 15 μm depending on when the error measurement is taken. Four cases appear to be clearly relevant in the situation. They correspond to the four dynamic error attributes identified in Fig. 4: the maximum positioning error (MPE) that appears immediately after the positioning acceleration, the residual positioning error (RPE) observed after the acceleration dissipation and defined by the average of a number of dynamic error values before deceleration, the maximum approaching error (MAE) observed immediately after the approaching acceleration and the residual approaching error (RAE) observed after some settling time between deceleration and probing.

3. Preliminary Experiments and Study

The experiments are carried out on a 3-axis moving bridge type coordinate measuring machine. The errors measurements are performed using an API laser system providing five simultaneous displacement measurements (linear displacement, horizontal straightness, vertical straightness, yaw, pitch and roll errors) as well as velocity and acceleration measurements.[26] It is important to note that all the conducted experiments are executed after the laser had been preheated in conformity to the precision standard. Moreover, these experiments were performed in a humidity and temperature (20°C) controlled environment. The experimental setup is illustrated in Fig. 5. During the experiments, the CMM moves at a high speed and a high acceleration

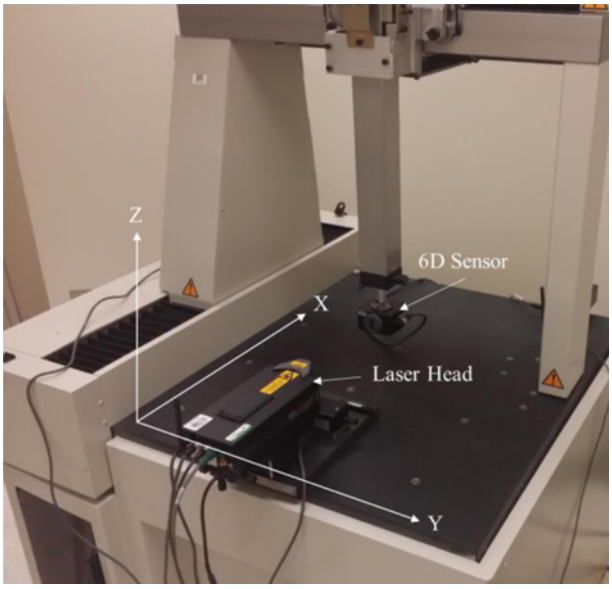

Fig. 5 Experimental setup

to exhibit the dynamic properties and the weak parts of the CMM.

The method of measuring the dynamic errors while the bridge is moving along the x-guideway is given as an example. With the x-carriage at a middle position along the beam (Y = 250 mm), the bridge moves in the x-direction at different speeds and accelerations. The variations of the velocity and the acceleration during the measurement process are assumed to be the largest contributors to the dynamic errors by means of the inertial forces produced in two stages: from start to the programmed velocity and from the programmed velocity to stop. Because all machine components have finite stiffness, they will endure deflections due to inertial forces resulting in rotation and translation errors at the joints. For this reason, it is essential to measure the variation caused by varied velocity and accelerations for the error components associated with the axis from start to stop.

The API laser system is then used to evaluate the dynamic translations and rotations in different directions. Fig. 6 shows typical results of dynamic characteristic measurement from start to stop using a positioning velocity of 40 mm/s, a positioning acceleration of 200 mm/s^2, a positioning distance of 40 mm, an approaching velocity of 12 mm/s, an approaching acceleration of 60 mm/s^2 and an approaching distance of 10 mm. It can be observed that all the dynamic error characteristics are correlated to the velocity. The biggest variation in these characteristics appears as acceleration and deceleration effects particularly in the case of angular errors. The horizontal and vertical straightness fluctuations reflect the possible friction between the air bearings and centrifugal forces induced by the motion pattern.

In order to establish a reference, measurement parameters are set at small values in such way that the effects of dynamic errors can be neglected. The measurement is repeated numerous times, and the results are recorded. Subsequently, the measurement parameters are changed to the desired values and the same measurements are performed. The differences between the recorded results represent the dynamic errors. Error compensation is only possible if and only if the dynamic errors are repeatable. The results indicate that the repeatability of the CMM

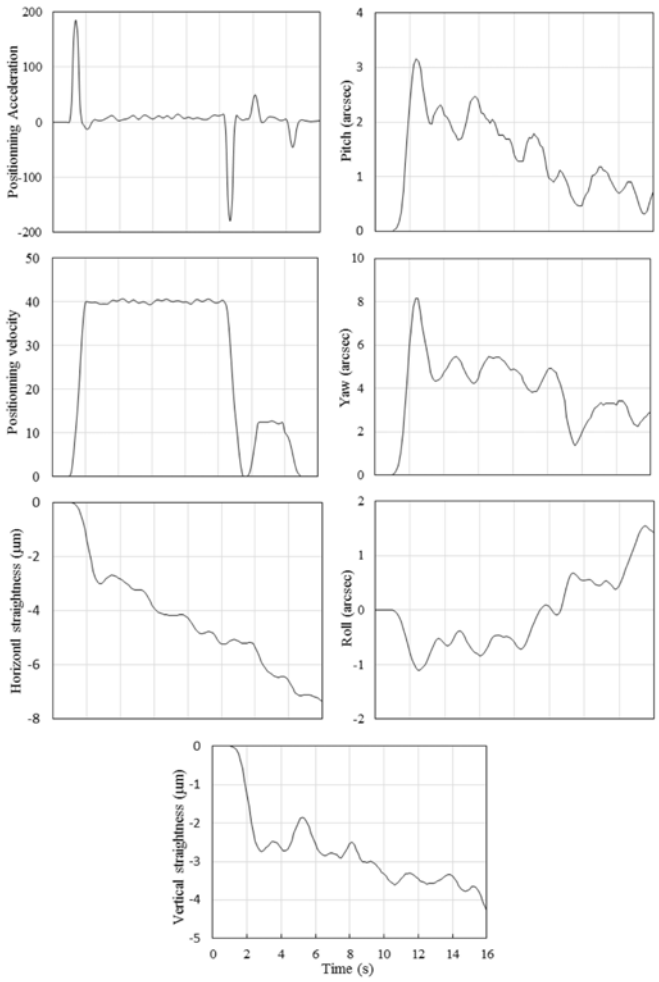

Fig. 6 Typical results of dynamic error characteristic measurement

Table 2 Basic repeatability check experience

Repetition	MPE (μm)	RPE (μm)	MAE (μm)	RAE (μm)
1	13.318	5.817	7.749	4.011
2	15.206	6.177	7.269	3.983
3	11.683	6.462	7.121	3.818
4	13.505	5.482	7.058	4.334
5	14.397	5.367	8.527	3.499
Min	11.683	5.367	7.058	3.499
Max	15.206	6.462	8.527	4.334
Average	13.622	5.861	7.545	3.929
St. deviation	1.321	0.461	0.612	0.304

when probing one point in the x direction is approximately 1 mm. In order to ensure the validity of the experimental results, a test selected randomly is repeated five times. The factor's levels for these experiments were set as follows: positioning velocity at 40 mm/s, positioning distance at 40 mm, approaching velocity at 12 mm/ and approaching distance at 10 mm. The results summarized in Table 2 present a very good repeatability. The variations are less than 10% (9.69, 7.87, 8.12 and 7.75% for MPE, RPE, MAE and RAE respectively). These results ensure the measurement method validity and prepare for modeling phase with confidence.

When the repeatability of the dynamic error is evaluated, an

Table 3 Maximum dynamic errors measured along different location along the y-transverse

Dynamic errors	y-carriage position (mm)		
	0 (left)	250 (middle)	500 (right)
MPE (μm)	11.957	13.622	22.619
RPE (μm)	5.137	5.861	10.291
MAE (μm)	7.473	7.544	12.196
RAE (μm)	4.272	3.928	7.543

investigation is conducted to estimate the dynamic error variations along the x axis with the y-carriage in different positions along the y-transverse (Fig. 3). Three positions were chosen: right (y = 500 mm), center (y = 250 mm) and left (y = 0 mm). The results are shown in Table 3, and demonstrate that when the y-carriage is at different locations along the y-transverse, the dynamic errors shows significant variation for MPE but only relatively limited changes for RPE, MAE and RAE. The yaw error is greater when the y-carriage travels from the left edge to the right one. This behavior mirrors a combinatory effect of the bending of the y-transverse and the torsion of the left support, along with the rotational error around the joints of the air bearings. It is important to note that investigation of these errors along the z or y axis was not performed since previous literature suggests that there are few changes in these errors due to firm conformity with Abbe principle. Also, before performing the proposed experimental design, a separate evaluation of the factor effects is achieved. In order to accomplish this, a one factor experiment is performed. It consists of an evaluation of the effect of one factor while ostensibly holding everything else constant. However, one disadvantage of this approach is that any interactions between different factors cannot be observed. The results are highlighted in Figs. 7 and 8 for MPE & RPE and MAE & RAE respectively.

First, the influence of the positioning velocity and acceleration on the maximum positioning error and the residual positioning error is investigated. With positioning velocity at 40 mm/s, 70 mm/s, and 100 mm/s, MPE & RPE are measured by changing the positioning acceleration and the positioning distance. The relationship of the two dynamic error attributes and the three positioning factors are shown in Fig. 7. The MPE and RPE relationships with the positioning velocity according to different positioning distance is shown in Fig. 7(a). This model suggests that both dynamic errors increase with the positioning velocity. The effect of positioning distance is limited to about 2-3 mm for RPE and insignificant for MPE. In Fig. 7(b), MPE and RPE are represented as a function of the positioning velocity and acceleration. In this case, the MPE increases much more with the positioning velocity than with the positioning acceleration. The impact of the acceleration is limited to less than 2 mm. Fig. 7(c) presents MPE and RPE variation as function of the positioning distance. When the positioning distance increases, the deformation and oscillation will be damped out easily. For this reason, the positioning distance has no impact on MPE as expected but affect RPE significantly. RPE is much less when the positioning distance is 80 mm than that when the distance is 30 mm.

The influence of the approaching velocity on the maximum approaching error and the residual approaching error is also investigated. MAE and RAE are measured with approaching velocity at 8, 12, and 16 mm/s and approaching distance at 5, 10 and 15 mm. Fig. 8 presents the relationships of MAE and RAE using the approaching velocity and

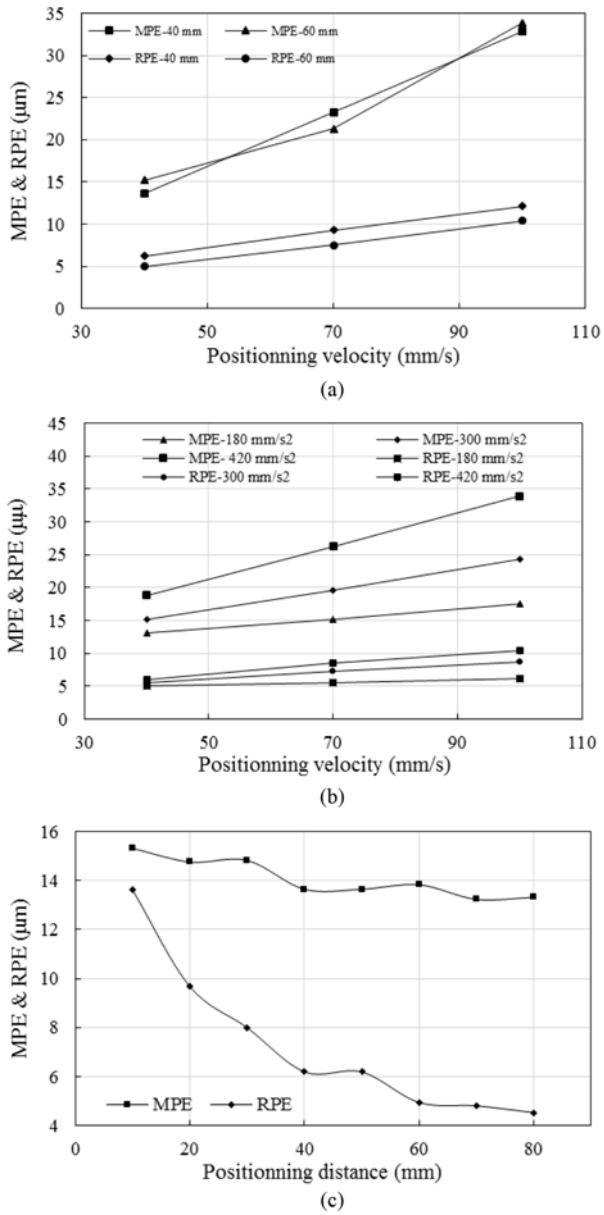

Fig. 7 Maximum and residual positioning dynamic errors under different parameters

distance as measuring factors. The relationships of the MAE and RAE with the approaching velocity according to different approaching distances is shown in Fig. 8(a). These results suggest that MAE and RAE increase significantly with the approaching velocity. When the approaching velocity is greater than 15 mm/s, a significant deformation is caused by the bending and MAE and RAE increase rapidly. These results are confirmed in Fig. 8(b) where the approaching distance is conserved constant at 10 mm. As confirmed in Fig. 8(c), where the approaching velocity is constant at 12 mm/s, the effect of the approaching distance is generally limited to less than 2 mm for RPE but can reach about 8 mm for RAE.

As the time and the accuracy of the measurement process are affected by the programmed motion pattern, it is essential to try to reduce the cycle time for improved productivity and therefore to compensate for the errors resulting from this process. The productivity improvement can

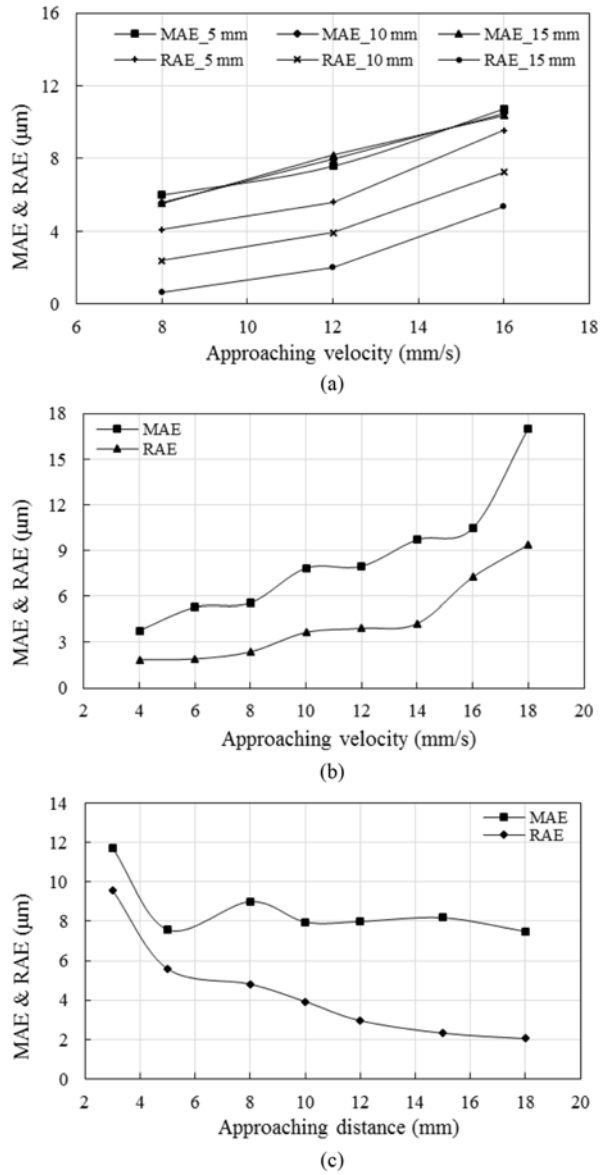

Fig. 8 Maximum and residual approaching dynamic errors under different parameters

be achieved by increasing the positioning velocity and the approaching velocity and by reducing the positioning distance and the approaching distance. However, it would be preferable to completely transform the motion pattern by keeping only one velocity (measuring velocity) and one distance (approaching distance) and try to optimize these variables in terms of accuracy and productivity according to specific applications.

This idea appears realistic and practical when one observes carefully the results obtained in the preliminary experiments. Indeed, the evolution of RPE and RAE as function of the velocity are comparable despite the fact that they are obtained at different accelerations. This suggests that the apparent cumulative effects of velocity and acceleration could be described using the velocity only. This is particularly plausible if the control parameters of the CMM are adapted to maintain constantly the acceleration proportional to the velocity (constant time to attain the target velocity). Accordingly, additional structured and comprehensive experimentations are conducted in order to assess the potential of this approach. The results of this experimentation are presented in the following section.

Table 4 Factors and levels for the experiments

Levels	PV (mm/s)	PD (mm)	AV (mm/s)	AD (mm)
1	40	40	8	5
2	70	60	12	10
3	100	-	16	15

4. Experimental design and analysis

As mentioned, numerous factors have an important influence on different dynamic error attributes. In order to illustrate the proposed investigation approach, this study use four relevant factors for characterizing the dynamic error attributes (MPE, RPE, MAE, RAE). These factors are related to the dynamic conditions of the measurement process: the positioning velocity (PV) in mm/s, the positioning distance (PD), the approaching velocity (AV) and the approaching distance (AD). The acceleration is not included among the factors in accordance with the assumption stating the apparent cumulative effects of velocity and acceleration.

4.1 Experimental design

In any experiment, the quality of the acquired data depends mainly on the data collection method. In a lot of cases, full factorial experiments are conducted. However, this design cannot be implemented when there are too many factors under consideration because the number of repetitions required would lead to prohibitive costs. By contrast, the use of a strategy such as orthogonal arrays (OAs), developed by Taguchi, can lead to an efficient and robust fractional factorial design of experiments that can collect all of the statistically significant data with the minimum possible number of repetitions.[27] Accordingly, OAs will be used in this paper for the design of experiment procedure.

Experiments are performed using an L_{18} orthogonal array and is executed according to the factor levels of each repetition. All factor levels are chosen within the range recommended by the manufacturer. The used factors are limited to represent real measurement conditions. Table 4 presents the chosen factors and levels for the experiments. Each experiment is replicated three times with the same combination of factors. The errors measurements are acquired and conditioned so that only the steady-state portions are retained. For each repetition, the min, max and mean error values are calculated. The mean values are considered to be the most representative. Replication and randomization are among the three essential design of experiments principles. The principal of blocking[27] is also important when running experiments. For instance, one would consider experiments run at noon and midnight as two different blocks due to the vast difference in temperature in the summer if the CMM is on the shop floor instead of in a controlled atmosphere. However, this was not needed since our CMM is in a controlled environment.

4.2 Analysis strategy

The experimental data is analyzed using three statistical tools: the graph of the average effect for each factor, the percent contribution of

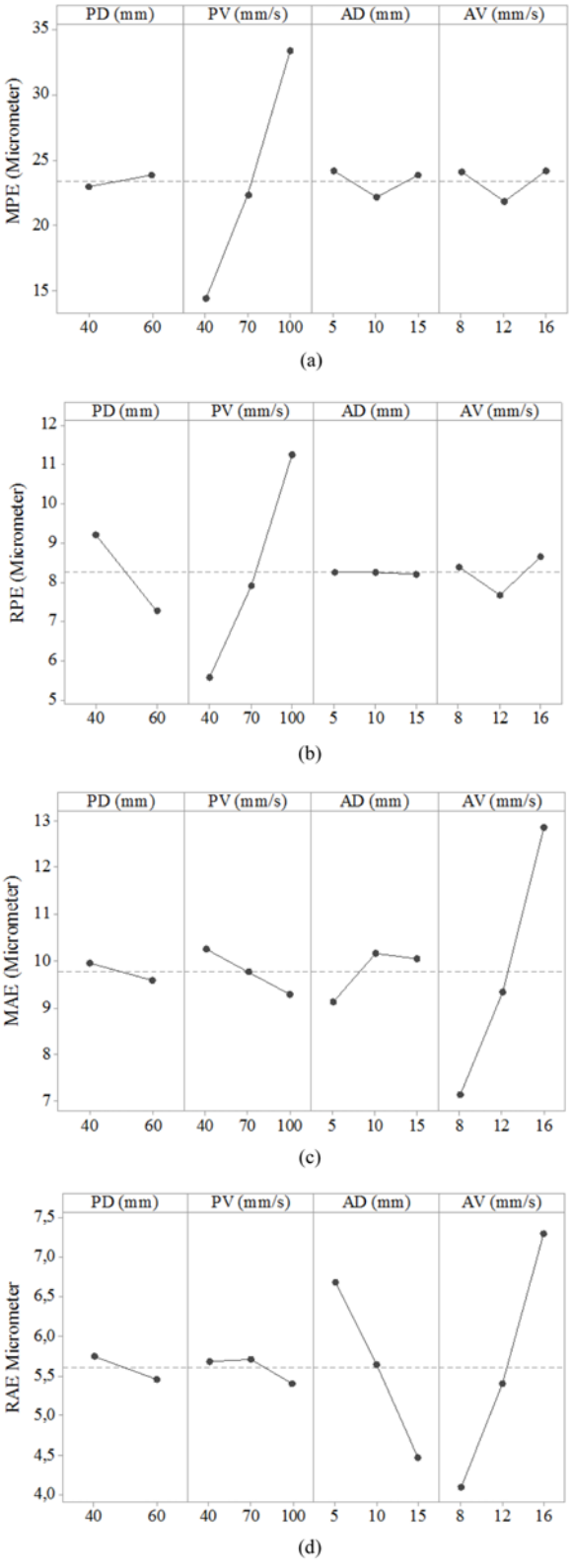

Fig. 9 Effects of measurement parameters on the dynamic error attributes

factors extracted from the analysis of variance (ANOVA) and the correlation between various dynamic error attributes and measurements factors. The percent contribution of a factor reflects the portion of the total variation observed in the experiment that is attributed to that factor.

Table 5 Percent contribution (%C) of measurement factors

	MPE		RPE		MAE		RAE	
	%C	F	%C	F	%C	F	%C	F
PD	0.28	0.54	13.6	27.85	0.49	0.42	0.80	1.05
PV	91.6	88.3	79.1	80.86	2.32	0.98	0.70	0.46
AD	1.15	1.11	0.01	0.010	3.25	1.38	29.1	19.2
AV	1.77	1.71	2.4	2.5	82.1	34.7	61.8	40.4
Error	5.19	-	4.89	-	11.8	-	7.6	-
Total	100	-	100	-	100	-	100	-

Ideally, the total percent contribution of all considered factors must add up to 100. Any difference from 100 represents the contribution of other uncontrolled factors and experimental errors. As the experiments are designed using an OA, the estimates of the average effect of a given factor on various responses will not be biased.

4.3 Experimental data analysis

Fig. 9 shows that various dynamic error attributes are affected at different degrees by measurement parameters. The factors most affecting MPE is PV. These results are expected, since MPE is observed immediately after positioning acceleration, which is recognized to have a significant effect on the machine dynamics. MPE is more sensitive to changes in the positioning velocity than to the positioning distance. The increase of the positioning distance helps in the dissipation of the acceleration effects. For this reason, PD appear with PV as the factors most affecting RPE. AV is the factor that have the most influence on MAE. This is due to the fact that MAE is observed immediately after the approaching acceleration which is strongly correlated to AV than to AD. However, AD plays an important role in the dissipation of the acceleration effects. RAE appears plausible as function of AV and AD.

Similar conclusions can be clearly established from the percent contributions analysis. Percent contribution and F-test values extracted from ANOVA and reported in Table 5 reveal that globally the four factors have an influence on the dynamic error. However, specific groups of factors have significant effects on specific dynamic error attributes. These results confirm the observations reported in Fig. 9. Thus, PV and AV contribute for more than 80% to the variation of MPE and MAE, which are strongly sensitive to the acceleration/deceleration. RPE and RAE observed after the dissipation of acceleration effects are less sensitive to PV and AV. PD an AD contribute for RPE and RAE by about 14 and 30%, respectively. The errors remain within acceptable levels (about 10%), implying that the most important measurement parameters influencing the dynamic error are all included in the experiments.

The correlation analysis results reported in Table 6 show that specific dynamic error attributes are correlated to specific measurement parameters. Using a minimum threshold of 25%, it is possible to identify the most relevant variables for an eventual modeling procedure. Accordingly, one can presume that MPE and MAE can be controlled using PV and AV, respectively. RPE can be controlled using PV and PD, while RAE can be controlled using AV and AD. These suppositions can be confirmed by the correlations between various dynamic error attributes. These conclusions suggest that there are many options to consider for building an efficient dynamic error prediction model for error compensation.

Table 6 Correlation analysis results between measurement factors and dynamic error attributes

Correlations	MPE	RPE	MAE	RAE
PD	0.0529	0.3689	0.0701	0.0893
PV	0.9526	0.8842	0.1521	0.0679
AD	0.0176	0.0045	0.1454	0.5411
AV	0.0048	0.0444	0.8982	0.7801
MPE	1	0.8931	0.1393	0.0526
RPE	-	1	0.0593	0.0107
MAE	-	-	1	0.7381
RAE	-	-	-	1

Several parameters affecting the dynamic errors of CMMs are identified. The dynamic error attributes exhibit a complex and nonlinear relationship with these parameters. To be able to implement an effective error compensation strategy, it is necessary to develop an efficient and robust model that can predict these errors accurately. Although several techniques can be used to produce such a model, artificial neural networks (ANN) have been proven to be an effective tool for this type of applications,[28-30] thus ANN is chosen in this study for an illustrative example of dynamic error prediction model.

As indicated before, only the dynamic errors when probing in the x direction are modeled using the ANN. The experimental data from the L_{18} design is used to train the ANN prediction model. In this modelling test, the y-carriage is considered at the central position and the variation in z direction is not taken into account. The proposed model is then referred to the x axis only. The experimentation results suggest that positioning and approaching velocity and distances are the largest contributor to the dynamic error variations. Consequently, PV, PD, AV and AD are used as input to the model.

Thus, when the CMM probes in the x direction, the dynamic error attributes are predicted with the model and also measured experimentally. The predicted values can be used to compensate for the real errors obtained from measurement. The measured and predicted dynamic errors are shown in Fig. 10 for various combination measurement parameters. These results demonstrate that the dynamic errors can be reduced by at least 80%. The results suggest that the modeling approach can be effective for dynamic error prediction and compensation. A more accurate definition of the dynamic error attributes, an experiment covering more factors and more levels for more training and validation data as well as an improvement of the modeling procedure can lead to more accurate and efficient models. This may probably lead to error reduction to levels that can exceed 95%. This will make it possible to use a higher velocity for an improved CMM productivity while maintaining the accuracy at very high levels.

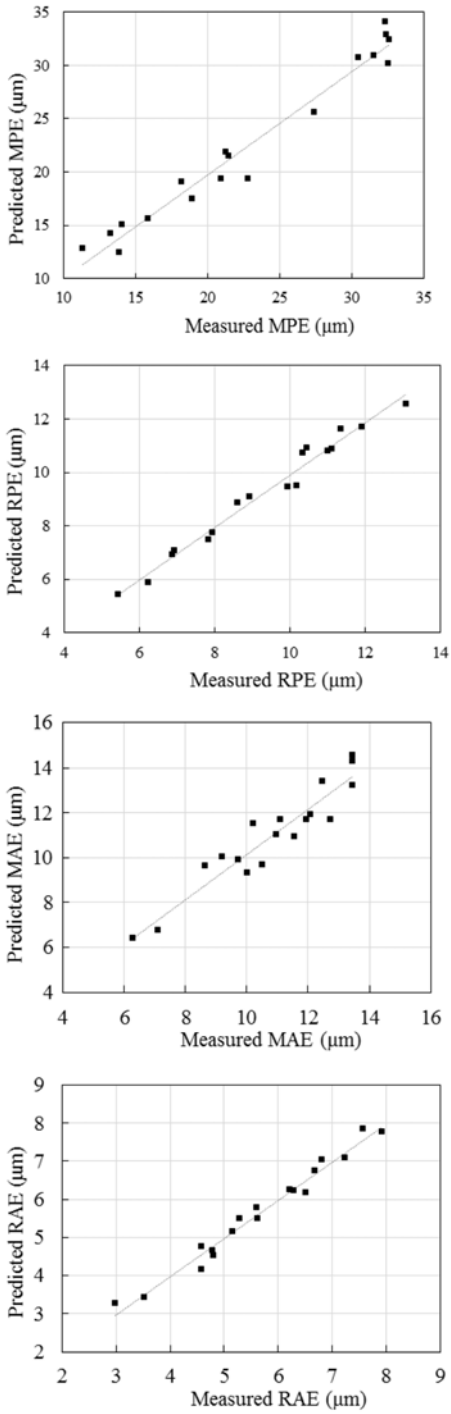

Fig. 10 Predictive modelling results for the dynamic error compensation model

5. Conclusion

In this study, the dynamic errors of CMMs are studied using a structured and comprehensive experimental approach. Several characteristics of the dynamic error that occur at the probe position in case of higher velocity measurement are evaluated under various measurement conditions. Relationships between dynamic translation and rotation errors, positioning accuracy, measurement parameters and deformations caused by inertia effects due to accelerations are identified. Consequently, four attributes of the dynamic error are defined in order to follow the error variations at different stages of the measurement pattern from start to stop and to understand how the measurement parameters affect these variations. Carried out on a bridge type CMM using a touch-trigger, the experimental investigation is based on positioning velocity, positioning distance, approaching velocity and approaching distance as measurement parameters to study the variation of maximum positioning error, residual positioning error, maximum

approaching error and residual approaching error as dynamic error attributes. The dynamic error components and the dynamic positioning errors at the probe position are evaluated under selected dynamic conditions using a laser interferometer system. The measurements of the error components are executed according to an efficient and structured experimental design. An error of less than 10% achieved in repeatability tests ensures that the measurements are consistent and robust.

Based on laser measurement and using various statistical analysis tools, the average effects of the measurement parameters and the effects of their interactions on different dynamic error attributes are analyzed. Their contributions in dynamic positioning error variations are evaluated. The experimental results show that the angular errors can have significant effects inducing more than 70% of dynamic positioning error, especially in a CMM with low stiffness. A multivariate analysis reveals that each dynamic error attribute is strongly correlated to a specific group of measurement parameters. Explicit and quantified criteria is used to identify the most relevant variables for consistent and practical predictive modeling. Confirmed by a multiple correlation analysis between dynamic error attributes and measurement parameters, the results suggest that many options can be considered for building an efficient dynamic error prediction model for error compensation. An artificial neural network based simplified predictive model is given as an example to demonstrate the possible and promising performance of error prediction and error compensation that can be achieved.

REFERENCES

1. Hammad Mian, S. and Al-Ahmari, A., "New Developments in Coordinate Measuring Machines for Manufacturing Industries," International Journal of Metrology & Quality Engineering, Vol. 5, No. 1, pp. 101-110, 2014.
2. Hocken, R. J. and Pereira, P. H., "Coordinate Measuring Machines and Systems," CRC Press, 2016.
3. Han, Z. Y., Jin, H. Y., Liu, Y. L., and Fu, H. Y., "A Review of Geometric Error Modeling and Error Detection for CNC Machine Tool," Applied Mechanics and Materials, Vols. 303-306, pp. 627-631, 2013.
4. Schwenke, H., Knapp, W., Haitjema, H., Weckenmann, A., Schmitt, R., and Delbressine, F., "Geometric Error Measurement and Compensation of Machines - An Update," CIRP Annals, Vol. 57, No. 2, pp. 660-675, 2008.
5. Mekid, S. and Ogedengbe, T., "A Review of Machine Tool Accuracy Enhancement through Error Compensation in Serial and Parallel Kinematic Machines," International Journal of Precision Technology, Vol. 1, Nos. 3-4, pp. 251-286, 2010.
6. Fan, J., Guan, J., Wang, W., Luo, Q., Zhang, X., and Wang, L., "A Universal Modeling Method for Enhancement the Volumetric Accuracy of CNC Machine Tools," Journal of Materials Processing Technology, Vol. 129, Nos. 1-3, pp. 624-628, 2002.
7. Aguado, S., Samper, D., Santolaria, J., and Aguilar, J. J., "Towards an Effective Identification Strategy in Volumetric Error Compensation of Machine Tools," Measurement Science and Technology, Vol. 23, No. 6, Paper No. 065003, 2012.
8. Choi, J., Min, B., and Lee, S., "Reduction of Machining Errors of a Three-Axis Machine Tool by On-Machine Measurement and Error Compensation System," Journal of Materials Processing Technology, Vol. 155, pp. 2056-2064, 2004.
9. Zhang, Z., and Hu, H., "A General Strategy for Geometric Error Identification of Multi-Axis Machine Tools Based on Point Measurement," The International Journal of Advanced Manufacturing Technology, Vol. 69, Nos. 5-8, pp. 1483-1497, 2013.
10. Barakat, N., Elbestawi, M., and Spence, A., "Kinematic and Geometric Error Compensation of a Coordinate Measuring Machine," International Journal of Machine Tools and Manufacture, Vol. 40, No. 6, pp. 833-850, 2000.
11. Tan, K. K., Huang, S. N., Lim, S. Y., Leow, Y. P., and Liaw, H. C., "Geometrical Error Modeling and Compensation Using Neural Networks," IEEE Transactions on Systems, Man, and Cybernetics, Part C (Applications and Reviews), Vol. 36, No. 6, pp. 797-809, 2006.
12. Zhu, S., Ding, G., Qin, S., Lei, J., Zhuang, L., and Yan, K., "Integrated Geometric Error Modeling, Identification and Compensation of CNC Machine Tools," International Journal of Machine Tools and Manufacture, Vol. 52, No. 1, pp. 24-29, 2012.
13. Kruth, J.-P., Vanherck, P., and Van Den Bergh, C., "Compensation of Static and Transient Thermal Errors on CMMs," CIRP Annals-Manufacturing Technology, Vol. 50, No. 1, pp. 377-380, 2001.
14. Ramesh, R., Mannan, M., and Poo, A., "Error Compensation in Machine Tools - A Review: Part II: Thermal Errors," International Journal of Machine Tools and Manufacture, Vol. 40, No. 9, pp. 1257-1284, 2000.
15. Yang, H. and Ni, J., "Dynamic Modeling for Machine Tool Thermal Error Compensation," Journal of Manufacturing Science and Engineering, Vol. 125, No. 2, pp. 245-254, 2003.
16. De Nijs, J., Lammers, M., Schellekens, P., and Van der Wolf, A., "Modelling of a Coordinate Measuring Machine for Analysis of Its Dynamic Behaviour," CIRP Annals-Manufacturing Technology, Vol. 37, No. 1, pp. 507-510, 1988.
17. Ricciardi, G., Borsati, L., and Micheletti, G., "Theoretic and Experimental Methodologies for Increasing Dynamic Performances of General Purpose Robots and Measuring Machines," CIRP Annals-Manufacturing Technology, Vol. 34, No. 1, pp. 375-379, 1985.
18. Weekers, W. G. and Schellekens, P. H. J., "Assessment of Dynamic Errors of CMMs for Fast Probing," CIRP Annals-Manufacturing Technology, Vol. 44, No. 1, pp. 469-474, 1995.
19. Dong, C., Zhang, C., Wang, B., and Zhang, G., "Prediction and Compensation of Dynamic Errors for Coordinate Measuring Machines," Journal of Manufacturing Science and Engineering, Vol. 124, No. 3, pp. 509-514, 2002.

20. Dong, C., Zhang, C., Wang, B., and Zhang, G., "Prediction and Compensation of Dynamic Errors for Coordinate Measuring Machines," Journal of Manufacturing Science and Engineering, Vol. 124, No. 3, pp. 509-514, 2002.

21. Dong, C., Zhang, C., Wang, B., and Zhang, G., "Reducing the Dynamic Errors of Coordinate Measuring Machines," Journal of Mechanical Design, Vol. 125, No. 4, pp. 831-839, 2003.

22. Mu, Y. H. and Ngoi, B. K. A., "Dynamic Error Compensation of Coordinate Measuring Machines for High-Speed Measurement," The International Journal of Advanced Manufacturing Technology, Vol. 15, No. 11, pp. 810-814, 1999.

23. Pereira, P. H. and Hocken, R. J., "Characterization and Compensation of Dynamic Errors of a Scanning Coordinate Measuring Machine," Precision Engineering, Vol. 31, No. 1, pp. 22-32, 2007.

24. Weekers, W. G. and Schellekens, P. H. J., "Compensation for Dynamic Errors of Coordinate Measuring Machines," Measurement, Vol. 20, No. 3, pp. 197-209, 1997.

25. Chang, D. and Spence, A., "CMM Dynamic Error Analysis, Control and Compensation," Proc. of the American Society for Precision Engineering Annual Meeting, 2007.

26. Laser Automated Precision Inc., "Measuring All 6 Degrees of Freedom - XD Laser" https://www.apisensor.com/measuring-6-degrees-freedom-xd-laser-automated-precision-inc/ (Accessed 9 JUL 2018)

27. Montgomery, D. C., "Design and Analysis of Experiments," John Wiley & Sons, 2017.

28. Huang, S. H. and Zhang, H.-C., "Artificial Neural Networks in Manufacturing: Concepts, Applications, and Perspectives," IEEE Transactions on Components, Packaging, and Manufacturing Technology: Part A, Vol. 17, No. 2, pp. 212-228, 1994.

29. Meireles, M. R., Almeida, P. E., and Simões, M. G., "A Comprehensive Review for Industrial Applicability of Artificial Neural Networks," IEEE Transactions on Industrial Electronics, Vol. 50, No. 3, pp. 585-601, 2003.

30. Dagli, C. H., "Artificial Neural Networks for Intelligent Manufacturing," Springer Science & Business Media, 2012.